Effects of ion mobility and positron fraction on solitary waves in weak relativistic electron-positron-ion plasma

Ding Lu, Zi-Liang Li, and Bai-Song Xie*
Key Laboratory of Beam Technology and Materials Modification of the Ministry of Education, and College of Nuclear Science and Technology, Beijing Normal University, Beijing 100875, China
(Received 14 July 2013; published 30 September 2013)

The effects of ion mobility and positron fraction on the solitary waves of the laser field envelope and the potential of the electrostatic field in weak relativistic electron-positron-ion plasma are investigated. The parameter region for the existence of solitary waves is obtained analytically, and a reasonable choice of parameters is clarified. Both cases of mobile and immobile ions are considered. It is found that the amplitudes of solitary waves in the former case are larger compared to the latter case. For small plasma density, the localized solitary wave solutions in terms of the approximate perturbation analytical method are very consistent with those by exact numerical calculations. However, as the plasma density increases the analytical method loses its validity more and more. The influence of the positron fraction on the amplitudes of solitary waves shows a monotonous increasing relation. The implications of our results to particle acceleration are also discussed briefly.

DOI: 10.1103/PhysRevE.88.033109 PACS number(s): 52.27.−h, 52.35.Mw, 52.35.Sb

I. INTRODUCTION

Since the relativistic laser-plasma interaction was first investigated by Akhiezer and Polovin [1], many nonlinear phenomena have been found, such as solitons, vortices, double layers and so on. In particular, the discovery of electromagnetic solitary waves have attracted the attention of many people due to its robust and resilient behaviors [2]. In past decades many works have been performed in conventional electron-ion (EI) plasma [3–7]. On the other hand, there exists also electron-positron-ion (EPI) plasma in most astrophysical environments and in the laboratory [8], for example, in the pulsar magnetosphere [9], the active galactic nuclei [10], and the early universe [11]. Recently, the studies of nonlinear waves in the intense laser field interacting with EPI plasma have revealed some new features [12–19]. Usually the EPI plasma is very different from the conventional EI plasma, and also different from the pure electron-positron (EP) plasma [13]. An obvious fact is that there are no soliton solutions for pure EP plasma because the charge density is cancelled for charge-neutralized electrons and positrons.

Let us recall some research that has been done regarding localized solitary wave solutions in two-component plasma, EI and/or EP, and three-component plasma, EPI. Farina and Bulanov [5,20] studied the relativistic electromagnetic solitons in EI and EP plasma. In our previous study we obtained the parameter region of existence of solitons and the bifurcation diagram for EI plasma [21]. Berezhiani *et al.* [4] studied the relativistic solitary waves in cold EP plasma in an external magnetic field. They also found the large-amplitude envelope solitons analytically in EPI plasma [14]. By using the reductive perturbation method, Mahmood *et al.* [22] obtained the small-amplitude Korteweg–de Vries (KdV) soliton solutions in hot EPI plasma and they also considered the influence of temperature ratio of electrons to positrons on solitons. Lehmann and Spatschek [23] studied the manifolds of periodic solutions by Poincaré section plots; they found that the ion dynamics strongly affects the structure of the phase plot and the ion motion must not be neglected in the high-intensity regime. Some other works have also been done, such as studies of ion-acoustic solitary waves [15] and vortices [16,17] in EPI plasma.

The propose of this paper is to investigate solitary waves in the cold and unmagnetized EPI plasma. We will focus on three important aspects. First we have to choose a set of parameters which are relatively practical and physical by the requirement of approximated wave dispersion. It is noted that this point has always been either omitted or less discussed in many previous publications. Second, we employ the numerical technique to solve the coupling equations of the laser field envelope and the potential of the plasma electrostatic field, which can provide an exact solitary wave solution. Third, we generalize the approximate perturbation analytic method developed by others [13] for the immobile ion case to the case including ion motion. Motivated by these factors, we study cases of both mobile and immobile ions. The numerical results are compared to the analytical ones. We also hope that our results in this paper are helpful to clarify the properties of nonlinear solitary waves in EPI plasma. Before giving the exact numerical solutions, we made a detailed stability analysis for the fixed point of the system and the parameter region for the existence of solitary waves, as in Ref. [21], which can give a relatively deeper understanding of nonlinear coherent structure in multicomponent plasma.

The paper is organized as follows. Section II reviews the theoretical model of laser-plasma interaction for the completeness of the paper, and presents the parameter region where solitary waves may exist analytically in terms of the nonlinear dynamics method. Section III exhibits the exact numerical solutions in cases of both mobile and immobile ions, and the numerical results are compared to the approximate analytical solutions. A conclusion is given in Sec. IV. Finally, the derivation of the analytical method by the perturbation

*Corresponding author: bsxie@bnu.edu.cn

series expansion technique generalized to the mobile-ion case is discussed in the Appendix.

II. THEORETICAL MODEL AND BASIC FORMALISM

The basic formalism of problem studied is certain from the Maxwell equations and hydrodynamic equations. In the following the physical quantities involved are normalized as time $\omega_\mathrm{p} t$, length $k_\mathrm{p} x$, potential $e\phi/m_e c^2$, electromagnetic fields $eE/m_e c\omega_\mathrm{p}$ and $eB/m_e c\omega_\mathrm{p}$, density n/n_{0e}, velocity v/c, and momentum $p/m_\alpha c$, respectively, where ω_p is the electron plasma frequency, m_e is the electron rest mass, and n_{0e} is the unperturbed electron density. Charges q_α are normalized to $-e$, where α indicates the particle species ($\alpha = e,p,i$), so for the electron $q_\mathrm{e} = 1$; for the positron and ion $q_\mathrm{p} = q_\mathrm{i} = -1$; ρ_α is defined as m_e/m_α; for the electron and positron $\rho_e = \rho_p = 1$; and for the ion (for simplicity we assumed it to be a proton) $\rho_\mathrm{i} = 1/1836$. We shall consider that the system is initially in an equilibrium state, which is characterized by $n_{0\mathrm{e}} = n_{0\mathrm{p}} + n_{0\mathrm{i}}$ to ensure the charge neutrality. The positron fraction can be defined as $\chi = n_{0\mathrm{p}}/n_{0\mathrm{e}}$, which is the ratio of positron to electron initially.

By using the normalized quantities mentioned above, the Maxwell equations and hydrodynamic equations are written as

$$\nabla^2 \boldsymbol{A} - \frac{\partial^2}{\partial t^2}\boldsymbol{A} - \frac{\partial}{\partial t}\nabla\phi = n_e \boldsymbol{v}_e - n_p \boldsymbol{v}_p - n_i \boldsymbol{v}_i, \quad (1)$$

$$\nabla^2\phi = n_e - n_p - n_i, \quad (2)$$

$$\frac{\partial n_\alpha}{\partial t} + \nabla\cdot(n_\alpha \boldsymbol{v}_\alpha) = 0, \quad (3)$$

$$\frac{\partial \boldsymbol{P}_\alpha}{\partial t} = \nabla(\rho_\alpha q_\alpha \phi + \gamma_\alpha) + \boldsymbol{v}_\alpha \times \nabla \times \boldsymbol{P}_\alpha, \quad (4)$$

where $\boldsymbol{P}_\alpha = \boldsymbol{p}_\alpha - \rho_\alpha q_\alpha \boldsymbol{A}$ is the canonical momentum, $\gamma_\alpha = \sqrt{1+|\boldsymbol{p}_\alpha|^2}$ is the relativistic factor, and $\boldsymbol{v}_\alpha = \boldsymbol{p}_\alpha/\gamma_\alpha$ is particle fluid velocity. Note that we have chosen the Coulomb gauge $\nabla\cdot\boldsymbol{A} = 0$.

As in most previous studies, for convenience, we consider only the problem where all the quantities vary only along the direction of propagation x. We look for the solution of vector potential as the form $\boldsymbol{A} = a(\xi)\exp(i\omega\tau)$, where the new variables $\xi = x - vt$, $\tau = t - vx$ are introduced and v is the laser group velocity. By the way, the wave traveling phase velocity is just $1/v$.

In the quasistatic approximation and the initial plasma conditions of $p_\alpha = 0$, $n_e = 1$, $n_p = \chi$, and $n_i = 1-\chi$ at infinity, we get the reduced coupling equations as follows:

$$\frac{d^2 a}{d\xi^2} = -\omega^2 a + a\mathcal{F}_1/\varepsilon^2 \equiv g(a,\phi), \quad (5)$$

$$\frac{d^2\phi}{d\xi^2} = \mathcal{F}_2/\varepsilon^2 \equiv h(a,\phi), \quad (6)$$

where $\varepsilon^2 = 1 - v^2$ (obviously $0 \leqslant \varepsilon \leqslant 1$) and two auxiliary quantities are introduced as

$$\mathcal{F}_1 = \sqrt{1-\varepsilon^2}\left[\frac{1}{R_e} + \frac{\chi}{R_p} + \frac{\rho_i(1-\chi)}{R_i}\right], \quad (7)$$

$$\mathcal{F}_2 = \sqrt{1-\varepsilon^2}\left[\frac{\psi_e}{R_e} - \frac{\chi\psi_p}{R_p} - \frac{(1-\chi)\psi_i}{R_i}\right], \quad (8)$$

with $\psi_\alpha = \rho_\alpha q_\alpha \phi + 1$ and $R_\alpha = \sqrt{\psi_\alpha^2 - (1-v^2)(1+\rho_\alpha^2 a^2)}$. Now Eqs. (5) and (6) constitute a set of coupled ordinary differential equations (ODEs) for the vector potential of the laser pulse and wake potential of plasma, which are our starting points for further investigations in the following.

We shall first discuss the nonlinear dynamics that is hidden in these equations. In order to predict the existence of the solitary waves, Eqs. (5) and (6) can be reduced to a set of one-order ODEs as $a' = b$, $b' = g(a,\phi)$, $\phi' = c$, $c' = h(a,\phi)$, where the prime indicates $d/d\xi$. The fixed points can be calculated from $b = 0$, $g(a,\phi) = 0$, $c = 0$, and $h(a,\phi) = 0$. For example, in the case of a mobile ion the fixed point $(a,a',\phi,\phi') = (0,0,0,0)$ is found. It is easy to find that the characteristic roots of the Jacobi determinant are $\lambda_{1,2}^2 = [1+\chi+\rho_i(1-\chi)]/\varepsilon^2 - \omega^2$ and $\lambda_{3,4}^2 = -[1+\chi+\rho_i(1-\chi)]/(1-\varepsilon^2)$. Let us denote $\delta = \varepsilon\omega$. Obviously, if $0 < \delta < \delta_c = \sqrt{1+\chi+\rho_i(1-\chi)}$, the characteristic roots are $\lambda_{1,2} = \pm\sqrt{[1+\chi+\rho_i(1-\chi)]/\varepsilon^2 - \omega^2}$ and $\lambda_{3,4} = \pm i\sqrt{[1+\chi+\rho_i(1-\chi)]/(1-\varepsilon^2)}$. Accordingly, the stability analysis mentioned above shows that the fixed point (0,0,0,0) is a saddle center when $0 < \delta < \delta_c$. This means that in this region solitary waves exist.

Because ions are much heavier than the electrons, the ion motion could be neglected for simplified treatment in some situations. Thus for the immobile ion case, similar to the mobile ion case, the coupling equations are in the same form except with $\rho_i = 0$, and with

$$\mathcal{F}_3 = \sqrt{1-\varepsilon^2}\left[\frac{1}{R_e} + \frac{\chi}{R_p}\right], \quad (9)$$

$$\mathcal{F}_4 = \sqrt{1-\varepsilon^2}\left[\frac{\psi_e}{R_e} - \frac{\chi\psi_p}{R_p} - \frac{(1-\chi)}{\sqrt{1-\varepsilon^2}}\right] \quad (10)$$

replacing the former $\mathcal{F}_1$ and $\mathcal{F}_2$. Similarly, we find that the fixed point is also (0,0,0,0) and the stability analysis shows that it is also the saddle center. The solitary waves can be available in the region of $0 < \delta < \delta_c = \sqrt{1+\chi}$.

III. RESULTS OF LOCALIZED SOLITARY WAVE SOLUTIONS

Before giving numerical and analytical solutions in the following, it is necessary to see how to choose the system parameters which are important for practical physical systems. It is well known that in a nonrelativistic frame we have the normalized laser group velocity $v = \sqrt{(1-\omega^{-2})}$ for conventional EI plasma. (Note that the normalized laser frequency is the ratio of real laser frequency ω_L to equilibrium plasma frequency ω_p, i.e., $\omega = \omega_L/\omega_p$.) This relation comes from the dispersion of transverse electromagnetic waves propagating in plasma. A further relation is that $\varepsilon^2 = 1 - v^2 = 1/\omega^2$, which will lead to $\delta = \varepsilon\omega = 1$. However, in the weakly relativistic frame, due to the plasma, mass is modified by the relativistic factor so that $\delta \approx 1/\gamma_e \lesssim 1$. Similarly, for EPI plasma we have $\delta \approx \delta_c/\gamma_e \lesssim \delta_c$ for both the mobile and immobile ion cases. These discussions lead to two facts. One is that the practical laser and plasma parameters can indeed lie in the region where the solitary waves can exist, analyzed in the last section. The other, maybe more important fact is that the production quantity $\delta = \varepsilon\omega$ should be near to the value of bifurcation point δ_c, because we are focusing on the weak

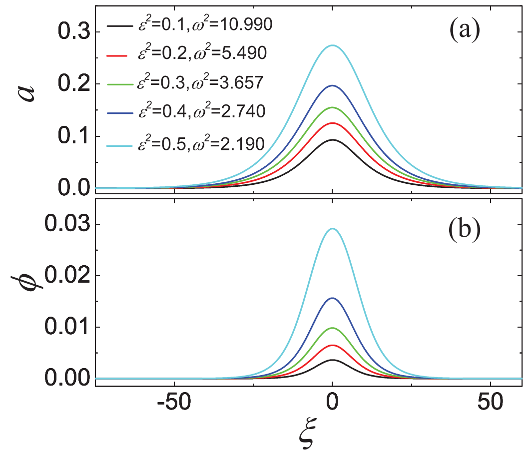

FIG. 1. (Color online) Solitary wave solutions of vector potential a in (a) and electrostatic potential ϕ in (b) for the mobile ion case. The positron fraction is $\chi = 0.1$, and the other parameters are seen in text.

relativistic problem in which the relativistical factor γ_e is a little larger than 1. In fact, our studies below support and confirm these analysis. We should remember that the larger parameter ε^2 ($\approx n/n_c$) corresponds to the higher plasma density but the smaller laser group velocity.

A. Effects of ion mobility

The fourth-order Runge-Kutta method is employed in our numerical techniques. We can find a series of numerical solitary wave solutions for Eqs. (5) and (6) with different parameters of ε and ω if χ is fixed. For illustration some typical numerical results are shown in Fig. 1 in the mobile ion case. Specifically, Fig. 1(a) is the envelope of vector potential a and Fig. 1(b) is the electrostatic potential ϕ. We have chosen $\chi = 0.1$ and five sets of ε and ω as $(\varepsilon^2,\omega^2) = (0.1,10.990)$ (black line), (0.2,5.490) (red line), (0.3,3.657) (green line), (0.4,2.740) (blue line), and (0.5,2.190) (cyan line). From the discussion mentioned above, these parameters are chosen to be near the bifurcation point, i.e., $\delta < \delta_c$ but $\delta_c - \delta \ll 1$. One can clearly see that with the increase of plasma density the amplitudes of solitary waves are increased accordingly in the mobile ion case. For the immobile ion case, we can get the corresponding solitary wave solutions in the same five sets of ε and ω, and the amplitudes of solitary waves increase also with the plasma density.

For comparison, the maximum values of vector potential and scalar potential in both the mobile (black squares) and immobile (red circles) ion cases are plotted in Fig. 2. It is found that the solitary wave amplitudes of vector potential a and electrostatic potential ϕ in the mobile ion case are always larger than that in the immobile ion case under the same conditions of ε, ω, and χ. This is not surprising, because only a stronger laser can excite the larger plasma motion, which causes the larger plasma potential. This self-consistent physical picture is a typical nonlinear characteristic in laser-plasma interaction, which is associated strongly with the ponderomotive force of the laser field as well as the electrostatic force due to plasma charge density.

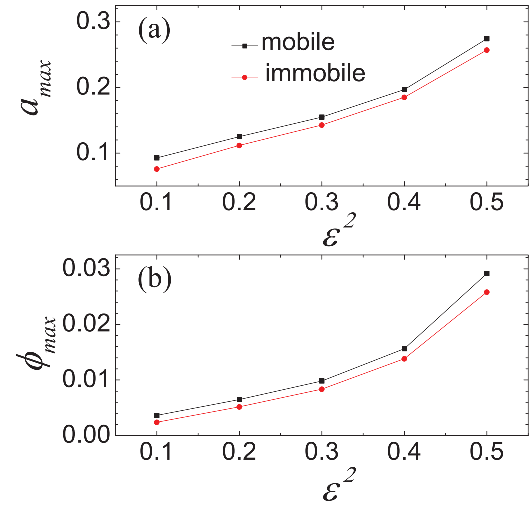

FIG. 2. (Color online) Maximum values of vector potential $a_{\max}$ and scalar potential $\phi_{\max}$ in mobile (black squares) and immobile (red circles) ion cases.

B. Comparison of numerical and analytical results

In order to compare the numerical solutions to analytical results, the derivation of analytical solutions is given in the Appendix. We get the concrete analytical expression for solitary wave solutions [Eq. (A17)] by using a similar perturbation series expansion method developed by others [13,24–27], but the scheme and results are generalized to include the ion dynamics.

Figure 3 demonstrates the maximum values of vector potential $a_{\max}$ and scalar potential $\phi_{\max}$ in both mobile (upper row) and immobile (lower row) ion cases with the numerical results (black square) and analytical results (red circles). The choice of system parameters is the same as in Fig. 1. One can find that as the plasma density ε^2 increases, the amplitudes of solitary waves a and ϕ increase monotonously

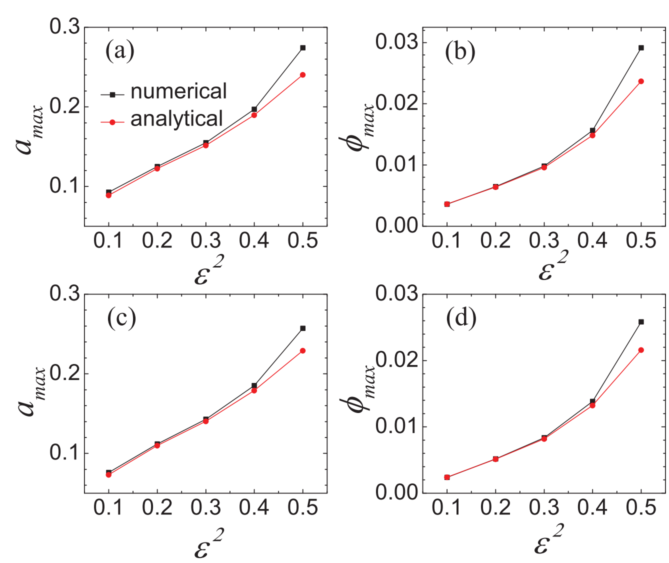

FIG. 3. (Color online) Maximum values of vector potential $a_{\max}$ and scalar potential $\phi_{\max}$ for the mobile ion case (upper row) and immobile ion case (lower row) by the numerical results (black squares) and analytical results (red circles).

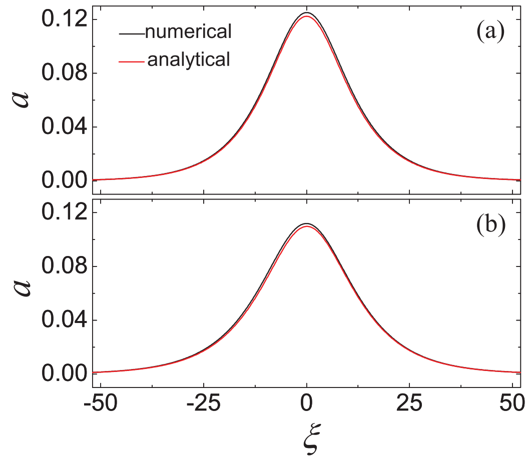

FIG. 4. (Color online) The numerical and analytical solutions of vector potential a for $\chi = 0.1$, $\varepsilon^2 = 0.2$, and $\omega^2 = 5.49$ in both the mobile ion case (upper row) and immobile ion case (lower row).

too. Meanwhile, the analytical results agree with the numerical results very well for small values of ε^2, i.e., a relatively tenuous plasma. However, as the plasma becomes dense enough, the underestimation of analytical solutions becomes more and more severe.

For the case of smaller plasma density, $\varepsilon^2 = 0.2$, and when parameters $\chi = 0.1$ and $\omega^2 = 5.49$ are given, the numerical and analytical solutions of vector potential a in both the mobile ion case (upper row) and immobile ion case (lower row) are shown in Fig. 4. The numerical solutions and the analytical ones are plotted by a black solid line and a red solid line, respectively. Indeed, the numerical results and analytical ones are almost the same, because the analytical expression is quite valid for the choice of parameters. On the other hand, for the higher plasma density $\varepsilon^2 = 0.5$ and given the other parameters as $\chi = 0.1$ and $\omega^2 = 2.19$, the corresponding numerical solutions and analytical solutions in both the mobile ion case (upper row) and immobile ion case (lower row) are shown in Fig. 5. Obviously, there are remarkable discrepancies between the numerical and analytical results. We think this is because the series expansion terms are not enough. If we take higher orders of terms in Eq. (A4), for example, $n = 3$ or $n = 4$, the analytical solutions will become more accurate, which will be in accordance with the numerical ones. These observations indicate that the limiting condition Eq. (A19) in the analytical method plays an important role. The series expansion would lose its validity rapidly if the convergence condition is violated, e.g., for the higher plasma density. Therefore the numerical solving scheme presented in this paper is necessary due to its exactness and simplicity compared to the analytical method.

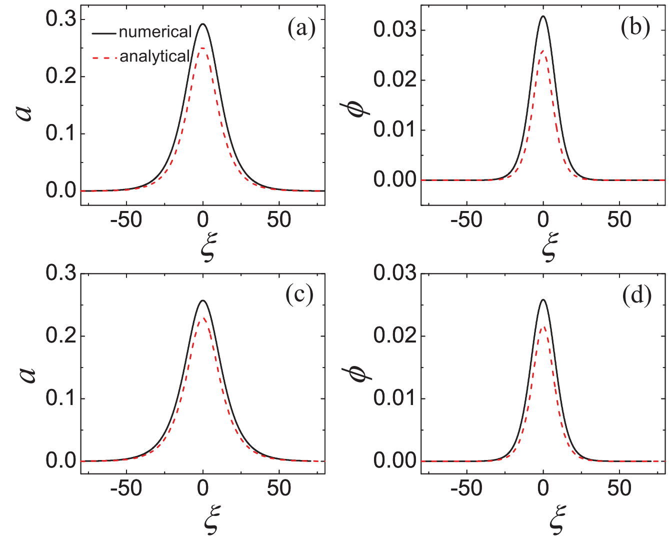

FIG. 5. (Color online) The numerical and analytical solutions of vector potential a and electrostatic potential ϕ for $\varepsilon^2 = 0.5$ and $\omega^2 = 2.19$ in both the mobile ion case (upper row) and immobile ion case (lower row).

monotonously, i.e., the ratio of positron to electron density can enhance the amplitudes of solitary waves. We also find the analytical results can fit the numerical results very well with small values of χ but deviate more and more as χ becomes large. Especially when χ lies in the region of $(1 - \chi) \ll 1$ (see Appendix), the analytical method will be severely invalid. Furthermore, by comparing the values of $a_{\max}$ and $\phi_{\max}$ in Fig. 6, we can find that the maximum values of a and ϕ in the mobile ion case are larger than those in the immobile ion case for the same parameters. These are simply the effects of ion dynamics on the solitary wave solutions.

C. Effects of positron fraction

To see the effect of positron fraction on solitary waves, we plot in Fig. 6 the maximum values of vector potential $a_{\max}$ and scalar potential $\phi_{\max}$ for the mobile ion case (upper row) and the immobile ion case (lower row) with the numerical results (black square) and analytical results (red circles). One can find that as χ increases both values of $a_{\max}$ and $\phi_{\max}$ are increased

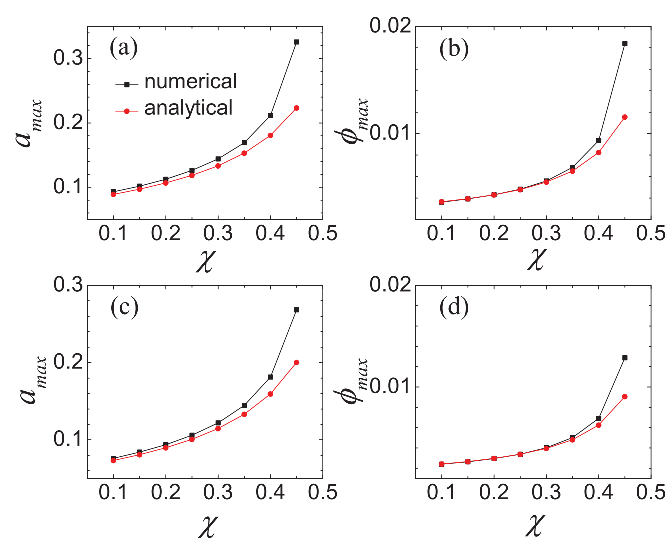

FIG. 6. (Color online) The numerical (black squares) and analytical (red circles) results of vector potential maximum values $a_{\max}$ and scalar potential maximum values $\phi_{\max}$ changing with χ for both the mobile ion (upper row) and immobile ion case (lower row) with parameter $\varepsilon^2 = 0.1$.

IV. CONCLUSIONS

In summary, in this paper the solitary waves have been found numerically and analytically in electron-positron-ion plasma with the condition of charge neutrality initially, and we have considered both mobile and immobile ions. The existence of solitary wave solutions has been found analytically in a certain parameter region. We also find that when an ion is mobile, compared to an immobile ion, both the parameter region and the amplitudes of solitary waves become larger. In addition, the positron concentration has a significant impact on the solitary waves in the considered plasma system. It is found that as the positron fraction increases, the parameter region of solitary waves becomes larger and the amplitudes of the waves as well. We also compare the numerical results with analytical solutions, and they are almost the same except for the cases of high plasma density and/or high positron fraction.

It is worthy to note that our research may be helpful to understand charged particle acceleration in plasmas. For example, the electrons can be accelerated from the bottom to reach the top in the wake plasma potential. The coupling between laser field a and wake field ϕ leads to a nonlinear localized structure such as the solitary waves presented in this paper, which would not only make the effective charged particle acceleration possible, but also opens a possible way to increase the acceleration efficiency through adjusting the system parameters, e.g., the plasma density and the positron fraction. This, however, is beyond the scope of the present paper and requires detailed study in the future.

ACKNOWLEDGMENTS

This work was supported by the National Natural Science Foundation of China (NNSFC) under Grants No. 11175023 and No. 11335013, and partially by the Fundamental Research Funds for the Central Universities (FRFCU). The computation was carried out at the HSCC of the Beijing Normal University.

APPENDIX: THE DERIVATION OF ANALYTICAL SOLUTION

By employing the series expansion method which was presented in Ref. [13], we calculate the analytical solutions of Eqs. (5) and (6). In this conservative system, it is not hard to find the integral of motion as

$$\begin{aligned}\left(\frac{da}{d\xi}\right)^2 - \frac{1}{\mathcal{R}}\left(\frac{d\phi}{d\xi}\right)^2 &= -\Omega\mathcal{A} - \frac{2v}{\mathcal{R}^2}\bigg(\sqrt{(1+\phi)^2-\mathcal{R}(1+\mathcal{A})} \\ &\quad + \chi(\sqrt{(1-\phi)^2-\mathcal{R}(1+\mathcal{A})} \\ &\quad + \frac{1-\chi}{\rho_i}\sqrt{(1-\rho_i\phi)^2-\mathcal{R}(1+\rho_i^2\mathcal{A})}\bigg) + E \\ &= \mathcal{H}(\phi,\mathcal{A}),\end{aligned} \tag{A1}$$

where $\mathcal{A}=a^2$, $\Omega=\omega^2$, $\mathcal{R}=\varepsilon^2$, and

$$E = \frac{2v^2}{\mathcal{R}^2}\left(1+\chi+\frac{1-\chi}{\rho_i}\right) \tag{A2}$$

is the integration constant which can be calculated from the boundary condition.

By using the energy integral and eliminating the independent variable ξ in Eqs. (5) and (6), we can get the following equation:

$$\begin{aligned}&4\mathcal{A}\mathcal{H}(\phi,\mathcal{A})\frac{d^2\phi}{d\mathcal{A}^2} - \frac{8}{\mathcal{R}}g(\phi,\mathcal{A})\mathcal{A}\left(\frac{d\phi}{d\mathcal{A}}\right)^3 \\ &\quad + \frac{4}{\mathcal{R}}\mathcal{A}h(\phi,\mathcal{A})\left(\frac{d\phi}{d\mathcal{A}}\right)^2 + 2[g(\phi,\mathcal{A})+\mathcal{H}(\phi,\mathcal{A})]\frac{d\phi}{d\mathcal{A}} \\ &\quad - h(\phi,\mathcal{A}) = 0.\end{aligned} \tag{A3}$$

We assume that the electrostatic field ϕ is the function of field amplitude $\mathcal{A}$ and use the series expansions as

$$\begin{aligned}\phi(\mathcal{A}) &= \sum_n c_n\mathcal{A}^n, \\ (1-\phi)^2-\mathcal{R}(1+\mathcal{A}) &= \sum_n a_n\mathcal{A}^n, \\ (1+\phi)^2-\mathcal{R}(1+\mathcal{A}) &= \sum_n b_n\mathcal{A}^n, \\ (1-\rho_i\phi)^2-\mathcal{R}(1+\rho_i^2\mathcal{A}) &= \sum_n d_n\mathcal{A}^n,\end{aligned} \tag{A4}$$

with $c_0=0$, $a_0=b_0=d_0=1-\mathcal{R}$. For $n \geqslant 1$, a_n, b_n, and d_n can be expressed by c_n as

$$\begin{aligned}&a_1 = -2c_1-\mathcal{R}, \quad a_2 = c_1^2-2c_2, \quad a_3 = 2c_1c_2-2c_3, \ldots \\ &b_1 = 2c_1-\mathcal{R}, \quad b_2 = c_1^2+2c_2, \quad b_3 = 2c_1c_2+2c_3, \ldots \\ &d_1 = -2\rho_ic_1-\rho_i^2\mathcal{R}, \quad d_2 = \rho_i^2c_1^2-2\rho_ic_2, \\ &d_3 = 2\rho_i^2c_1c_2-2\rho_ic_3, \ldots\end{aligned} \tag{A5}$$

We also assume the following expansions are valid:

$$\begin{aligned}&[(1-\phi)^2-\mathcal{R}(1+\mathcal{A})]^{\pm\frac{1}{2}} = v^{\pm1}\left(1 \pm \frac{1}{2v^2}\sum_n a_n\mathcal{A}^n\right), \\ &[(1+\phi)^2-\mathcal{R}(1+\mathcal{A})]^{\pm\frac{1}{2}} = v^{\pm1}\left(1 \pm \frac{1}{2v^2}\sum_n b_n\mathcal{A}^n\right), \\ &\left[(1-\rho_i\phi)^2-\mathcal{R}\left(1+\rho_i^2\mathcal{A}\right)\right]^{\pm\frac{1}{2}} = v^{\pm1}\left(1 \pm \frac{1}{2v^2}\sum_n d_n\mathcal{A}^n\right).\end{aligned} \tag{A6}$$

By inserting Eqs. (A4) and (A6) into Eq. (A3), we have

$$\begin{aligned}&-4\Omega\sum_{n=1} n(n-1)c_n\mathcal{A}^n - \frac{4}{\mathcal{R}^2}\sum_{n=1}\left(b_n+\chi a_n+\frac{1-\chi}{\rho_i}d_n\right)\mathcal{A}^{n+1}\sum_{n=1} n(n-1)c_n\mathcal{A}^{n-2} \\ &\quad - \frac{8}{\mathcal{R}}\left[\frac{1+\chi+\rho_i(1-\chi)}{\mathcal{R}}-\Omega\right]\mathcal{A}^2\left(\sum_{n=1} nc_n\mathcal{A}^{n-1}\right)^3 + \frac{4}{v^2\mathcal{R}^2}\sum_{n=1}[b_n+\chi a_n+\rho_i(1-\chi)d_n]\mathcal{A}^{n+2}\left(\sum_{n=1} nc_n\mathcal{A}^{n-1}\right)^3\end{aligned}$$

$$
\begin{aligned}
&+\frac{4}{\mathcal{R}^2}\left\{-\frac{1}{2v^2}\sum_{n=1}[b_n-\chi a_n-(1-\chi)d_n]\mathcal{A}^{n+1}+[1+\chi+\rho_i(1-\chi)]\sum_{n=1}c_n\mathcal{A}^{n+1}\right.\\
&\left.-\frac{1}{2v^2}\sum_{n=1}c_n\mathcal{A}^{n+1}\sum_{n=1}[b_n+\chi a_n+\rho_i(1-\chi)]\mathcal{A}^n\right\}\left(\sum_{n=1}nc_n\mathcal{A}^{n-1}\right)^2+2\left\{\left[\frac{1+\chi+\rho_i(1-\chi)}{\mathcal{R}}-2\Omega\right]\mathcal{A}\right.\\
&\left.-\frac{1}{\mathcal{R}^2}\sum_{n=1}\left(b_n+\chi a_n+\frac{1-\chi}{\rho_i}d_n\right)\mathcal{A}^n-\frac{1}{2v^2\mathcal{R}}\sum_{n=1}[b_n+\chi a_n+\rho_i(1-\chi)d_n]\mathcal{A}^{n+1}\right\}\sum_{n=1}nc_n\mathcal{A}^{n-1}\\
&-\frac{1}{\mathcal{R}}\left\{[1+\chi+\rho_i(1-\chi)]\sum_{n=1}c_n\mathcal{A}^n-\frac{1}{2v^2}\left[\sum_{n=1}[b_n-\chi a_n-(1-\chi)d_n]\mathcal{A}^n+\sum_{n=1}c_n\mathcal{A}^n\sum_{n=1}[b_n+\chi a_n+\rho_i(1-\chi)]\mathcal{A}^n\right]\right\}=0,
\end{aligned}
\tag{A7}
$$

and by using Eqs. (A5) and (A7), we can get the first two expansion coefficients of ϕ, i.e., c_1 and c_2:

$$c_1=\frac{\mathcal{R}(1-\chi)(1-\rho_i^2)}{2(4-3\mathcal{R})[1+\chi+\rho_i(1-\chi)]-8\mathcal{R}(1-\mathcal{R})\Omega}, \tag{A8}$$

$$c_2=c_1\kappa_1/\kappa_2, \tag{A9}$$

where

$$
\begin{aligned}
\kappa_1=&\frac{[(1-3\rho_i^2)c_1-2\mathcal{R}\rho_i^3-\rho_i](1-\chi)-\mathcal{R}(1+\chi)}{2\mathcal{R}(1-\mathcal{R})}\\
&+\frac{2c_1\{2(1+\chi)c_1+(1-\chi)[2\rho_ic_1-\mathcal{R}(1-\rho_i^2)]\}}{\mathcal{R}^2(1-\mathcal{R})}\\
&+\frac{6[1+\chi+(1-\chi)\rho_i]-8\mathcal{R}\Omega}{\mathcal{R}^2}c_1^2,
\end{aligned}
\tag{A10}
$$

$$\kappa_2=\frac{[1+\chi+(1-\chi)\rho_i](16-15\mathcal{R})}{\mathcal{R}(1-\mathcal{R})}-16\Omega. \tag{A11}$$

As $g(\phi(\mathcal{A}),\mathcal{A})\equiv g(\mathcal{A})$, Eq. (5) can be written as

$$2\mathcal{A}\left(\frac{d^2\mathcal{A}}{d\xi^2}\right)-\left(\frac{d\mathcal{A}}{d\xi}\right)^2-4\mathcal{A}g(\mathcal{A})=0, \tag{A12}$$

and its first integral is

$$\frac{1}{\mathcal{A}}\left(\frac{d\mathcal{A}}{d\xi}\right)^2-4\int\frac{g(\mathcal{A})}{\mathcal{A}}d\mathcal{A}=\text{const}=0. \tag{A13}$$

By expanding $g(\mathcal{A})$ with Eqs. (A4) and (A6), Eq. (A13) can then be reduced to

$$
\begin{aligned}
\left(v\frac{d\mathcal{A}}{d\xi}\right)^2=&4v^2\left[\frac{1+\chi+\rho_i(1-\chi)}{\mathcal{R}}-\Omega\right]\mathcal{A}^2\\
&-\frac{2}{\mathcal{R}}\sum_{n=1}\frac{b_n+\chi a_n+\rho_i(1-\chi)d_n}{n+1}\mathcal{A}^{n+2}.
\end{aligned}
\tag{A14}
$$

With a limit of $n\leqslant 2$, Eq. (A14) becomes

$$\left(v\frac{d\mathcal{A}}{d\xi}\right)^2=\alpha_1\mathcal{A}^2+\alpha_2\mathcal{A}^3+\alpha_3\mathcal{A}^4, \tag{A15}$$

where

$$
\begin{aligned}
\alpha_1&=\frac{4(1-\mathcal{R})}{\mathcal{R}}[1+\chi+\rho_i(1-\chi)-\mathcal{R}\Omega],\\
\alpha_2&=1+\chi+\rho_i^3(1-\chi)-\frac{2(1-\rho_i^2)(1-\chi)}{\mathcal{R}}c_1,\\
\alpha_3&=-\frac{2}{3\mathcal{R}}\{[1+\chi+\rho_i^3(1-\chi)]c_1^2+2(1-\rho_i^2)(1-\chi)c_2\}.
\end{aligned}
\tag{A16}
$$

For $\alpha_1>0$, the solution of Eq. (A15) is

$$\mathcal{A}=\frac{\beta_+\beta_-\text{sech}^2(\sigma\xi)}{\beta_+-\beta_-\tanh^2(\sigma\xi)}, \tag{A17}$$

where

$$
\begin{aligned}
\sigma&=\frac{\sqrt{\alpha_1}}{2v},\\
\beta_\pm&=\frac{-\alpha_2\pm\sqrt{\alpha_2^2-4\alpha_1\alpha_3}}{2\alpha_3}.
\end{aligned}
\tag{A18}
$$

As the argument in Ref. [13], for R satisfying

$$\left|c_4\mathcal{A}_{\max}^4\right|\leqslant\left|c_3\mathcal{A}_{\max}^3\right|\ll\left|c_1\mathcal{A}_{\max}+c_2\mathcal{A}_{\max}^2\right|<1, \tag{A19}$$

the series Eq. (A4) converged so rapidly that the solution Eq. (A17) is almost the same as the exact one (see Fig. 4).

Furthermore, from $\alpha_1>0$, we can get

$$0<\mathcal{R}<\frac{1+\chi+\rho_i(1-\chi)}{\Omega}, \tag{A20}$$

which is the same region as we have with the nonlinear dynamics method. So to keep the series expansion method valid, the range of values for $\mathcal{R}$ must satisfy Eqs. (A19) and (A20). Also, when $(1-\chi)\ll 1$, this analytical method is invalid.

Finally, it is noted that when $\rho_i=0$, the above solution can be recovered to the case of an immobile ion, which has been studied in Ref. [13].

[1] A. I. Akhiezer and R. V. Polovin, Sov. Phys. JETP **3**, 696 (1956).
[2] G. B. Whitham, *Linear and Nonlinear Waves* (Wiley, New York, 1974).
[3] S. V. Bulanov, T. Z. Esirkepov, N. M. Naumova, F. Pegoraro, and V. A. Vshivkov, Phys. Rev. Lett. **82**, 3440 (1999).
[4] V. I. Berezhiani, V. Skarka, and S. Mahajan, Phys. Rev. E **48**, R3252 (1993).
[5] D. Farina and S. V. Bulanov, Phys. Rev. Lett. **86**, 5289 (2001).
[6] B. S. Xie and S. C. Du, Phys. Plasma **13**, 074504 (2006).
[7] B. S. Xie and S. C. Du, Phys. Scr. **74**, 638 (2006).
[8] H. Chen, S. C. Wilks, J. D. Bonlie, E. P. Liang, J. Myatt, D. F. Price, D. D. Meyerhofer, and P. Beiersdorfer, Phys. Rev. Lett. **102**, 105001 (2009).
[9] F. C. Michel, Rev. Mod. Phys. **54**, 1 (1982).
[10] M. C. Begelman, R. D. Blandford, and M. D. Rees, Rev. Mod. Phys. **56**, 255 (1984).
[11] P. A. Sturrock, Astrophys. J. **164**, 529 (1971).
[12] V. I. Berezhiani, D. D. Tskhakaya, and P. K. Shukla, Phys. Rev. A **46**, 6608 (1992).
[13] V. I. Berezhiani, M. Y. El-Ashry, and U. A. Mofiz, Phys. Rev. E **50**, 448 (1994).
[14] V. I. Berezhiani and S. M. Mahajan, Phys. Rev. Lett. **73**, 1110 (1994); Phys. Rev. E **52**, 1968 (1995).
[15] S. I. Popel, S. V. Vladimirov, and P. K. Shukla, Phys. Plasma **2**, 716 (1995).
[16] P. K. Shukla, A. A. Mamun, and L. Stenflo, Phys. Scr. **68**, 295 (2003).
[17] Q. Haque and H. Saleem, Phys. Scr. **69**, 406 (2004).
[18] H. Kakati and K. S. Goswami, Phys. Plasma **7**, 808 (2000).
[19] M. K. Mishra, R. S. Tiwari, and S. K. Jain, Phys. Rev. E **76**, 036401 (2007).
[20] D. Farina and S. V. Bulanov, Phys. Rev. E **64**, 066401 (2001).
[21] C. C. Hua, B. S. Xie, and K. F. He, Chaos, Solitons Fractals **25**, 1161 (2005).
[22] S. Mahmood and H. Ur-Rehman, Phys. Lett. A **373**, 2255 (2009).
[23] G. Lehmann and K. H. Spatschek, Phys. Rev. E **83**, 036401 (2011).
[24] R. K. Varma and N. N. Rao, Phys. Lett. A **79**, 311 (1980).
[25] N. N. Rao and R. K. Varma, J. Plasma Phys. **27**, 95 (1982).
[26] N. N. Rao, R. K. Varma, P. K. Shukla, and M. Y. Yu, Phys. Fluids **26**, 2488 (1983).
[27] A. U. Mofiz and U. De Angelis, J. Plasma Phys. **33**, 107 (1985).